High-temperature superconductivity in LaH_{10}

D. A. Papaconstantopoulos, M. J. Mehl, and P.-H. Chang

Phys. Rev. B **101**, 060506 — Published 26 February 2020

DOI: 10.1103/PhysRevB.101.060506

High temperature superconductivity in LaH_{10}

D. A. Papaconstantopoulos*
Department of Computational and Data Sciences, George Mason University, Fairfax VA 22030

M. J. Mehl†
Center for Materials Genomics, Duke University, Durham NC 27708

P.-H. Chang‡
Department of Physics, University of Texas El Paso, El Paso TX 79902

(Dated: February 4, 2020)

The recent discovery of high critical temperature T_c in compressed H_3S has been followed by the prediction of Liu *et al.* of $T_c \approx 250\,K$ in the clathrate LaH_{10} structure. This report has been confirmed experimentally by Somayazulu *et al.* and Drozdov *et al.* Additional theoretical work by Wang *et al.* and Quan *et al.* further established the mechanism of electron-phonon interaction and the dominant role of hydrogen. In the present work we follow the classic McMillan paper, which separates the electron and phonon contributions to the electron-phonon coupling λ. We first compute the numerator of McMillan's expression, the Hopfield parameter η, using the theory of Gaspari and Gyorffy(GG), and obtain the force constants in the denominator from Wang *et al.* and Quan *et al.* The resulting λ is used in the Allen-Dynes equation to calculate T_c. The value of T_c reaches a maximum in the range of 236K-263K at pressures of 255 GPa and decreases for smaller or larger pressures. We provide a thorough analysis of the different terms of the GG equation and draw the conclusion that the sp channel of the hydrogen is the most important contribution to obtain high values of T_c in this material. Consistent with Wang *et al.* we find large values of λ that decrease with increasing pressure. In addition, we find that the hydrogen sites are the largest contributors to the total value of the coupling constant λ. That is, the acoustic mode associated with La contributes only 2% to the total λ, while the optic modes associated with H contribute 18% for the H1 site and 80% for the H2 site. These relative contributions to λ,are consistent to those given by Wang *et al.* and by Quan *et al.* Thus, our results strongly support the view that LaH_{10} is a metallic hydrogen superconductor.

I. INTRODUCTION

The high temperature superconductivity of about 200 K predicted by Duan *et al.*[1] at extreme pressures above 200 GPa in H_3S in the $Im\bar{3}m$ crystal structure,[2] and the immediate experimental confirmation by Drozdov *et al.*[3], has motivated numerous theoretical and experimental studies.[4–21] There is a strong consensus that conventional BCS electron-phonon coupling is the operating mechanism. The H_3S results led to the discovery of other hydride materials displaying even higher superconducting temperatures at high pressure. Prominent among those is the near room temperature (RT) superconductivity prediction of Liu *et al.*[7,15] for LaH_{10}.

The idea of metallization of hydrogen that was proposed long ago by Wigner and Huntington[22] and Ashcroft's prediction[23] of RT superconductivity in metallic hydrogen under high pressures is getting close to reality. After Ashcroft's prediction, Papaconstantopoulos and Klein[24] used the Gaspari-Gyorffy (GG) theory[25] to calculate electron-phonon coupling $\lambda = 1.86$ and superconducting temperature $T_c = 234\,K$ at a pressure of 460 GPa for metallic hydrogen. Unfortunately, metallization of pure hydrogen may require a pressure as high as 500 GPa.[26] The metal hydrides are thus an interesting alternative since they form metallic states at much lower pressures.

A special characteristic of the hydrides is the separation of the acoustic and optical phonon modes. The role of the metallic element (*e.g.* S or La) is to stabilize the material in a particular structure, but it is the hydrogen metallic states which are responsible for superconductivity.[27] After the prediction of Liu *et al.*, experimental papers by Somayazulu *et al.*[28] and Drozdov *et al.*[15] confirmed superconductivity with T_c over 250 K in LaH_{10}. Wang *et al.*[29] and Quan *et al.*[30] followed this with more theoretical work. In the present work on LaH_{10} we used the phonon frequencies from Wang *et al.* and Quan *et al.* and calculated the McMillan-Hopfield parameter η using the Gaspari-Gyoffy theory to gain further insights on the electron-phonon coupling and T_c in this material.

II. COMPUTATIONAL DETAILS

Superconducting LaH_{10} has a clathrate structure with $Im\bar{3}m$ symmetry. The electronic structure calculations were performed with the all-electron Linearized Augmented Plane Wave (LAPW) method,[31] specifically the Wei-Krakauer-Singh code,[32] developed at the U. S. Naval Research Laboratory. The present calculations use the Hedin-Lundqvist form of the local density approximation.[33] We set $RK_{\max} = 8.0$, and the muffin-tin radii $R_{\rm La}$=2.0 bohr and $R_{\rm H}$=1.0 bohr. Local orbitals were used for the La site. To ensure sufficient accuracy

for convergence, the total and orbital-projected densities of electronic states (pDOS) are calculated by the tetrahedron method with a uniformly distributed k-point grid of 505 k-points in the fcc irreducible Brillouin zone.

The key step to estimate T_c is the determination of the electron-phonon coupling λ, which, as pointed out by McMillan[34] and Hopfield[35], can be written as

$$\lambda_j = \frac{\eta_j}{M_j \left\langle \omega_j^2 \right\rangle} = \frac{N(E_F) \left\langle I_j^2 \right\rangle}{M_j \left\langle \omega_j^2 \right\rangle} \tag{1}$$

where $N(E_F)$ is the total DOS per spin at the Fermi level E_F, $\left\langle I^2 \right\rangle$ is the electron–ion matrix element, $\left\langle \omega_j^2 \right\rangle$ is the average phonon frequency and the index j corresponds to lanthanum or hydrogen. The Hopfield parameter η_j, which only describes electronic properties, is calculated using the GG formula based on scattering theory. This formula allows us to express the electronic contributions to the λ_j in local terms in the following form:

$$\eta_j = \frac{1}{N(E_F)} \sum_{l=0}^{2} 2(l+1) \sin^2(\delta_l^j - \delta_{l+1}^j) v_l^j v_{l+1}^j \tag{2}$$

where both δ_l^j and $v_l^j = N_l^j(\epsilon_F)/N_l^{j(1)}$ are orbital l and site j dependent. The phase shifts δ_l^j are defined through the following equation:

$$\tan \delta(R_s, E_F) = \frac{j_l' - j_l(kR_s) L_l(R_s, E_F)}{n_l' - n_l(kR_s) L_l(R_s, E_F)} \ , \tag{3}$$

where $k = \sqrt{E_F}$ in atomic units, $L_l = u_l'/u_l$ is the logarithmic derivative, and j_l and n_l are spherical Bessel and Neumann functions. The free scatterer DOS $N_l^{j(1)}$ is defined as follows:

$$N_l^{j(1)} = (2l+1) \int_0^{R^{\mathrm{MT}}} \left[u_l^j(r, E_F) \right]^2 r^2 dr \tag{4}$$

where u_l is the radial wave function and the upper limit of the integral is the muffin-tin radius R^{MT} for each atom.

Finally, T_c is evaluated using the Allen-Dynes equation[36] as follows:

$$T_c = f_1 f_2 \frac{\omega_{\log}}{1.2} \exp\left[-\frac{1.04(1+\lambda)}{\lambda - \mu^\star(1+0.62\lambda)} \right] \ , \tag{5}$$

with λ being the sum of the individual atomic values:

$$\lambda = \lambda_{\mathrm{La}} + 2\lambda_{\mathrm{H1}} + 8\lambda_{\mathrm{H2}} \ . \tag{6}$$

Here λ_{La} represents the acoustic modes associated with lanthanum atom, and λ_{H1} and λ_{H2} are the contributions from the optical modes of the two types of hydrogen atoms. This separation is exact for these materials and was pointed out a long time ago for other hydrides.[37] We have set the Coulomb pseudopotential $\mu^* = 0.13$. f_1 is the strong coupling factor,

$$f_1 = \left[1 + \left(\frac{\lambda}{2.46 + 9.35\mu^\star} \right)^{1.5} \right]^{1/3} \ , \tag{7}$$

FIG. 1: Pressure versus volume for LaH_{10} using the LAPW calculations described in the text.

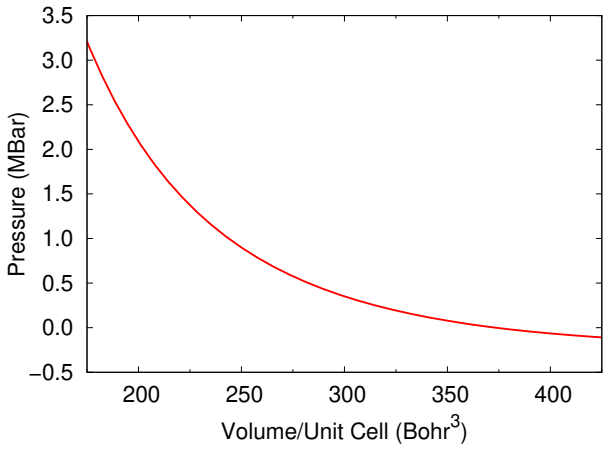

and f_2 is the "shape correction" of Allen and Dynes:[36]

$$f_2 = 1 + \left(\frac{\langle \omega \rangle (\mathrm{H})}{\omega_{\log}} - 1 \right) \frac{\lambda^2}{\lambda^2 + Y^2} \ . \tag{8}$$

where

$$Y = 1.82(1 + 6.3\mu^*) \frac{\langle \omega \rangle (\mathrm{H})}{\omega_{\log}}. \tag{9}$$

The values of $\langle \omega \rangle (\mathrm{H})$ and $\omega_{\log}$ are given in Table IV.

III. RESULTS AND ANALYSIS

Figure 1 shows pressure versus volume for LaH_{10}, calculated from a Birch fit to our LAPW calculations. Zero pressure corresponds to an equilibrium volume of 370.385 bohr^3 or a lattice parameter $a = 11.4$ bohr In our study we concentrate in a range of lattice constants from 8.7 bohr to 9.3 bohr, corresponding to pressures from 385 GPA to 205 GPa, the range where this material exhibits very high superconducting transition temperature.

In Figure 2 and Figure 3 we show the energy bands and densities of states for LaH_{10} at the lattice constant $a = 9.0$ bohr or pressure $P = 283$ GPa. Comparing these two graphs with those of Wang *et al.* we find very good agreement, despite the differences in the exchange and correlation functionals used in the two approaches. Both methods show metallic behavior and project very similar Fermi surfaces and overall occupied band width of approximately 25 eV. The DOS plot shows that the Fermi level is slightly above a van-Hove singularity, characteristic of these superconductors under pressure. In Figure 3 we have also plotted the site and angular momentum decomposed DOS. We note the stronger overall contribution of the La p-states away from E_f. Figure 3 also shows that the largest contribution to the DOS at E_f is from

FIG. 2: Band structure of LaH_{10} at the lattice constant $a = 9.0$ bohr, corresponding to a pressure of 283 GPa. The Fermi level is indicated by the solid horizontal line at 0.0 Ry. Calculations were performed with the LAPW code as described in the text.

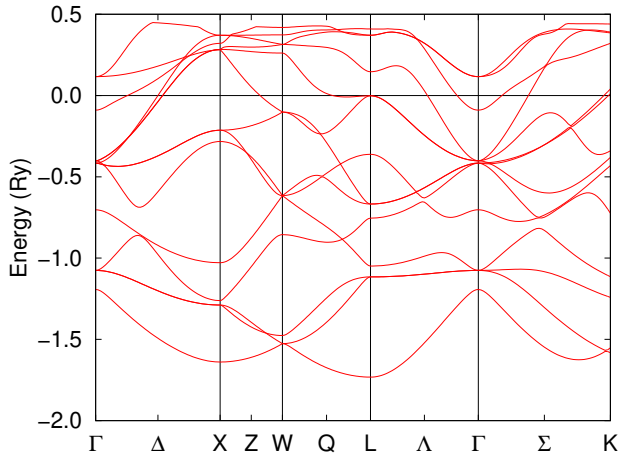

FIG. 3: Total and angular-momentum decomposed electronic density of states for LaH_{10} $a = 9.0$ bohr, corresponding to a pressure of 283 GPa. The Fermi level is indicated by the dashed vertical line at 0.0 Ry. Calculations were performed with the LAPW code as described in the text.

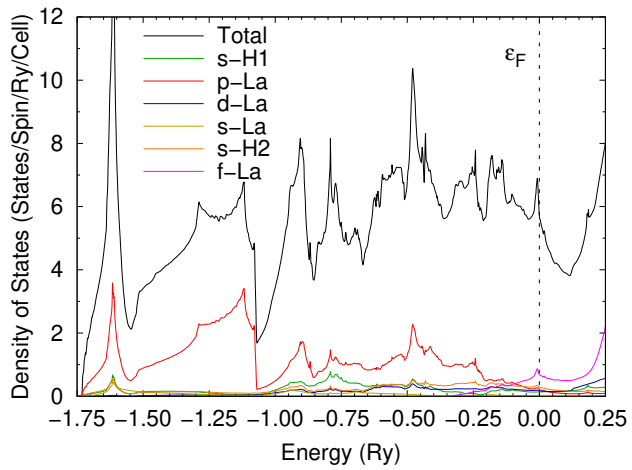

the f-like contribution of the La states. This is due to hybridization with the very high density of La f-states at about 0.4 Ry above E_f. As we discuss below this large value of the La DOS at E_f does not have a role in the calculation of the electron-phonon coupling which determines superconductivity. The important quantities in understanding superconductivity in this material are the s-like values of the hydrogen components of the DOS and not the p- and d-like La components.

The exact values of the angular momentum components of the DOS at E_f are listed in Table I for different lattice parameters and corresponding pressures per one spin.

It should be noted here that we have multiplied the

TABLE I: Density of states N and angular momentum components of the DOS at the Fermi level for LaH_{10} as a function of the lattice constant and pressure, in states/Ry/spin. The hydrogen partial densities of states are presented per site and are multiplied by a factor x=1.6 to correct for the small electron charge of approximately 0.5 electrons inside the muffin-tin spheres found in the LAPW calculations.

a (bohr)	P(GPa)	N(E_f)	s	p	d	f
			States/Ry/spin			
8.7	385	5.514				
		La	0.010	0.286	0.167	0.734
		H1	0.124	0.067	0.005	0.000
		H2	0.265	0.038	0.004	0.000
8.8	348	5.560				
		La	0.009	0.254	0.167	0.733
		H1	0.124	0.065	0.005	0.000
		H2	0.265	0.037	0.004	0.000
8.9	315	5.645				
		La	0.009	0.231	0.169	0.694
		H1	0.134	0.077	0.006	0.000
		H2	0.285	0.043	0.004	0.000
9.0	283	5.727				
		La	0.008	0.209	0.171	0.685
		H1	0.136	0.076	0.005	0.000
		H2	0.288	0.042	0.004	0.000
9.1	255	5.822				
		La	0.008	0.193	0.173	0.674
		H1	0.139	0.075	0.005	0.000
		H2	0.291	0.041	0.004	0.000
9.2	229	5.916				
		La	0.007	0.179	0.174	0.665
		H1	0.141	0.073	0.005	0.000
		H2	0.294	0.040	0.004	0.000
9.3	205	6.013				
		La	0.007	0.167	0.176	0.652
		H1	0.144	0.072	0.004	0.000
		H2	0.297	0.039	0.003	0.000

ℓ-components of the hydrogen DOS by a factor x=1.6 and reduced by the same amount the f-La DOS. The motivation for this correction comes from the realization that due to the geometry of the clathrate structure the LAPW calculation is done with very small muffin-tin spheres which results in unphysically small electron charge of about 0.5 electrons inside the hydrogen spheres. In addition, in the LAPW method there is an uncertainty on the position of the f-states which has led to the LDA+U correction. We view our redistributing the f-states of La and the H states as an empirical adjustment to mimic LDA+U. From Table I we observe that with increasing lattice constant, or decreasing pressure, $N(E_f)$ increases by about 9%, while the s-hydrogen component for the H2 site increase by about 12%. It is also noteworthy that the p-La DOS increases with increasing pressure by about 70% while the d-La DOS decreases by 6% with increasing pressure. However, we shall see later that while the H DOS is important for superconductivity the La-DOS has no role on superconductivity other than stabilizing the crystal structure.

To study the superconducting properties of this ma-

TABLE II: Hopfield parameter η (in eV/Å^2) and $\langle I^2\rangle$ (in (eV/Å)^2) for each atom type from (2) as a function of lattice constant a (in bohr) and pressure P (in GPa).

a	P	η La	η H1	η H2	$\langle I^2\rangle$ La	$\langle I^2\rangle$ H1	$\langle I^2\rangle$ H2
8.7	385	0.862	1.188	1.378	2.128	2.933	3.402
8.8	348	0.782	1.170	1.339	1.912	2.861	3.274
8.9	315	0.735	1.205	1.351	1.771	2.904	3.255
9.0	283	0.683	1.196	1.328	1.634	2.861	3.177
9.1	255	0.646	1.196	1.305	1.509	2.794	3.049
9.2	229	0.611	1.191	1.284	1.405	2.738	2.952
9.3	205	0.582	1.189	1.262	1.317	2.690	2.855

TABLE III: Contributions to the Hopfield parameter η and $\langle I^2\rangle$ per atom for the three channels in units of eV/Å^2 and (eV/Å)^2 respectively for lattice constant $a = 9.0$ bohr and $P = 283$ GPa.

	η-*sp*	η-*pd*	η-*df*	η-tot	$\langle I^2\rangle$-*sp*	$\langle I^2\rangle$-*pd*	$\langle I^2\rangle$-*df*
La	0.059	0.566	0.058	0.683	0.140	1.344	0.138
H1	1.186	0.010	0.000	1.196	2.817	0.024	0.000
H2	1.324	0.004	0.000	1.328	3.145	0.010	0.000

terial we start with the classic McMillan equation (1) in Section II, which separates the electron and phonon contributions to the electron-phonon coupling. We first calculate the numerator of (1), the Hopfield parameter "η" defined in (2), the Gaspari-Gyorffy (GG) formula. The results are shown in Table II. We note that, in the range of pressures that we have chosen, η(La) increases by about 48%. On the other hand η(H1) remains almost constant with increasing pressure while η(H2) increases by 9%. Although the per-atom values of η are smaller for La by only about a factor of two, we should stress here that we have 10 hydrogens in this structure which we will take into account in computing the parameter λ. In Table II we also list the values of $\langle I^2\rangle$ and note that the H1 shows an increase of 9% with pressure and H2 site shows an increase of 19%. This is to be contrasted with the 9% decrease of the N(E_f) shown in Table I. To provide further insights from the values of η shown in Table II we examine the GG formula (2) and we note that the summation for $\ell = 0, 1, 2$ has three terms, which we call the *sp*, *pd*, and *df* channels. We have found the largest contributors to these channels are the La-*pd* channel and the H-*sp* channels for both H sites. In Table III below we show the results for the lattice constant $a = 9.0$ bohr We found similar results for the rest of the lattice constants/pressures indicating the strength of the La-*pd* and the H-*sp* channels. We also found that in the H-*sp* channel, which gives the strongest contribution to the value of η, the $\sin^2$ term and the DOS product term $v_l^j v_{l+1}^j$ contribute about equally.

We now turn to the determination of the denominator of (1), the force constants $M\langle\omega^2\rangle$. We do this by interpolation/extrapolation of the phonon frequencies given by Wang *et al.* and Quan *et al.* We list these in Table IV.

Using the Hopfield parameters η and the force constants $M\langle\omega^2\rangle$ listed on Tables III and IV we can now compute the electron-phonon coupling constants $\lambda(j)$ for all three sites of LaH_{10}. The results are shown on Table V, where we multiply the H-components of λ by two and eight respectively to account for the number of crystallographic sites. Also on Table V we list the superconducting temperatures calculated by the Allen-Dynes formula (5) in our Section II Our results are given for two values of the H-DOS multiplier x=1.5 and 1.6.

Given the fact that we have used the Allen-Dynes equation and not the Eliashberg equations, our results for T_c are consistent with those of Wang *et al.* . We also in agreement with the experiments of Drozdov *et al.* and of Somayazulu *et al.* in which T_c reaches a maximum and decreases for lower and higher pressures. An important finding of this work that can be extracted from Table V is that the contribution of La to the total value of λ is negligible in comparison to the H contribution. This is consistent with the view that LaH_{10} is a metallic hydrogen superconductor. Also from Table V and Figure 4 we note that we have the same trend for λ_{tot} and ω_{log} as Wang *et al.*, that is ω_{log} increases with pressure while λ_{tot} decreases. We suggest that the difference in the maximum

TABLE IV: Averaged phonon frequencies from Wang *et al.* and Quan *et al.*

a	P	$\langle\omega\rangle$(La)	$\langle\omega\rangle$(H)	$\omega_{\log}$	$M\langle\omega^2\rangle$(La)	$M\langle\omega^2\rangle$(H)
bohr	GPa	K	K	K	eV/Å^2	eV/Å^2
8.7	385	324.	2264.	1905.	25.904	9.177
8.8	348	314.	2053.	1679.	24.329	7.546
8.9	315	306.	1869.	1483.	23.105	6.254
9.0	283	298.	1691.	1293.	21.913	5.120
9.1	255	291.	1536.	1127.	20.896	4.224
9.2	229	285.	1391.	784.	20.043	3.464
9.3	205	279.	1258.	467.	19.208	2.834

FIG. 4: LaH_{10} superconducting transition temperature T_c and λ_{tot} versus pressure using the $x = 1.5$ and $x = 1.6$ values from Table V.

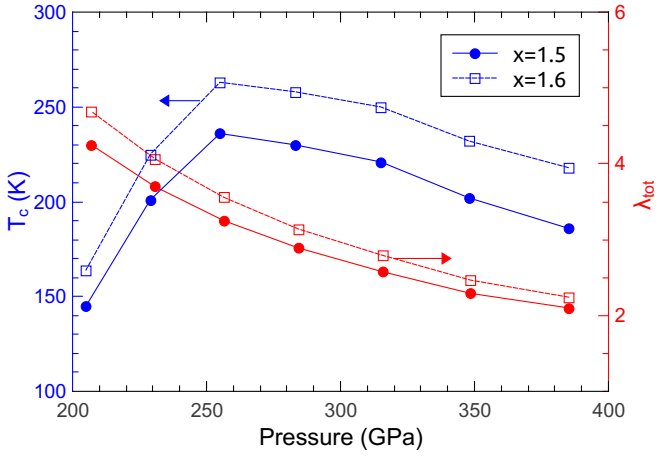

TABLE V: Electron-phonon coupling constant λ, prefactors f_1 and f_2 of the Allen-Dynes equation and superconducting temperature T_c. The Coulomb pseudopotential is set to $\mu^* = 0.13$. As indicated in Table I, we have multiplied the ℓ-components of the hydrogen atoms found inside the LAPW muffin-tins by the factor x, and decreased the f component of the lanthanum muffin-tin by the same amount.

		x=1.5							x=1.6						
a	P	λ(La)	λ(H1)	λ(H2)	$\lambda_{\rm tot}$	f_1	f_2	T_c	λ(La)	λ(H1)	λ(H2)	$\lambda_{\rm tot}$	f_1	f_2	T_c
Bohr	GPa							K							K
8.7	385	0.03	0.23	1.06	1.32	1.07	1.02	186	0.03	0.26	1.20	1.49	1.08	1.02	218
8.8	348	0.03	0.27	1.25	1.55	1.08	1.03	202	0.03	0.31	1.42	1.76	1.10	1.04	232
8.9	315	0.03	0.34	1.52	1.89	1.11	1.04	221	0.03	0.39	1.73	2.15	1.13	1.05	250
9.0	283	0.03	0.41	1.82	2.27	1.14	1.07	230	0.03	0.47	2.08	2.57	1.17	1.08	258
9.1	255	0.03	0.50	2.17	2.70	1.18	1.10	236	0.03	0.57	2.47	3.07	1.21	1.11	263
9.2	229	0.03	0.60	2.61	3.24	1.22	1.18	201	0.03	0.69	2.97	3.68	1.26	1.22	225
9.3	205	0.03	0.74	3.13	3.90	1.28	1.27	145	0.03	0.84	3.56	4.43	1.32	1.33	164

Tc of 236K and 263K for our parameter x=1.5 and x=1.6 respectively is within the accuracy of the approximations usually made in such calculations given the exponential form of the Allen-Dynes equation.

IV. CONCLUSIONS

We have performed LAPW band structure calculations to apply the Gaspari-Gyorffy theory for determining the Hopfield parameter η. We have combined these with published results of the phonon frequencies to calculate the electron-phonon coupling and the superconducting transition temperature T_c for LaH_{10}. The results for η, accounting for the ten hydrogen sites in the structure, make the H contribution 20 times stronger a=9.1 Bohr than that from La. Due to the much larger force constant of La, which makes the λ(La) small, this conclusion of the dominance of the hydrogen sites is retained and even strengthened. Thus, the acoustic modes associated with La contribute only 2% to the total value λ, in contrast to the optic modes associated with hydrogen which contribute 18% and 80% for the H1 and H2 sites respectively. Our results are in very good agreement regarding the high values of T_c obtained by experiment and other theoretical works. The concept that LaH_{10} is a metallic hydrogen superconductor is strongly supported.

Acknowledgments

This work was partially supported by the U.S. Department of Energy grant DE-SC0014337 and by the Alliance for Sustainable Energy.

* dpapacon@gmu.edu
† michael.mehl@duke.edu
‡ chang.pohao@gmail.com

[1] D. Duan, Y. Liu, F. Tian, D. Li, X. Huang, Z. Zhao, H. Yu, B. Liu, W. Tian, and T. Cui, Scientific Reports **4**, 30 (2014).
[2] D. Hicks, M. J. Mehl, E. Gossett, C. Toher, O. Levy, R. M. Hanson, G. Hart, and S. Curtarolo, Computational Materials Science **161**, S1 (2019), URL `http://www.aflowlib.org/CrystalDatabase/A3B_cI8_229_b_a.html`.
[3] A. P. Drozdov, M. I. Eremets, I. A. Troyan, V. Ksenofontov, and S. I. Shylin, Nature **525**, 73 (2015).
[4] F. Fan, D. A. Papaconstantopoulos, M. J. Mehl, and B. M. Klein, Journal of Physics and Chemistry of Solids **99**, 105 (2016).
[5] J. A. Flores-Livas, A. Sanna, and E. K. Gross, European Physical Journal B **89**, 52 (2016).
[6] Y. Ge, F. Zhang, and Y. Yao, Physical Review B **93**, 1 (2016).
[7] H. Liu, I. I. Naumov, R. Hoffmann, N. W. Ashcroft, and R. J. Hemley, Proceedings of the National Academy of Sciences **114**, 6990 (2017).
[8] D. A. Papaconstantopoulos, M. J. Mehl, and H. Liu, Quantum Studies: Mathematics and Foundations (2017).
[9] D. A. Papaconstantopoulos, Novel Superconducting Materials **3**, 29 (2017).
[10] S. Zhang, Y. Wang, J. Zhang, H. Liu, X. Zhong, H. F. Song, G. Yang, L. Zhang, and Y. Ma, Scientific Reports **5**, 1 (2015).
[11] X. Zhong, H. Wang, J. Zhang, H. Liu, S. Zhang, H. F. Song, G. Yang, L. Zhang, and Y. Ma, Physical Review Letters **116**, 1 (2016).
[12] C. Heil and L. Boeri, Physical Review B **92**, 1 (2015).
[13] M. Mahdi Davari Esfahani, Z. Wang, A. R. Oganov, H. Dong, Q. Zhu, S. Wang, M. S. Rakitin, and X.-F. Zhou, Scientific Reports **6**, 22873 (2016).
[14] T. Matsuoka, M. Hishida, K. Kuno, N. Hirao, Y. Ohishi, S. Sasaki, K. Takahama, and K. Shimizu, Physical Review B **99**, 144511 (2019).
[15] A. P. Drozdov, P. P. Kong, V. S. Minkov, S. P. Besedin, M. Kuzovnikov, S. Mozaffari, L. Balicas, F. F. Balakirev, D. E. Graf, V. B. Prakapenka, et al., Nature **569**, 528 (2019).
[16] N. Bernstein, C. S. Hellberg, M. D. Johannes, I. I. Mazin, and M. J. Mehl, Physical Review B **91**, 060511 (2015).
[17] E. J. Nicol and J. P. Carbotte, Physical Review B **91**, 220507 (2015).
[18] R. Akashi, M. Kawamura, S. Tsuneyuki, Y. Nomura, and

R. Arita, Physical Review B **91**, 224513 (2015).
[19] D. A. Papaconstantopoulos, B. M. Klein, M. J. Mehl, and W. E. Pickett, Physical Review B **91**, 1 (2015).
[20] F. Peng, Y. Sun, C. J. Pickard, R. J. Needs, Q. Wu, and Y. Ma, Physical Review Letters **119**, 107001 (2017).
[21] P.-H. Chang, S. Silayi, D. A. Papaconstantopoulos, and M. J. Mehl, Journal of Physics and Chemistry of Solids (2019), in press.
[22] E. Wigner and H. B. Huntington, The Journal of Chemical Physics **3**, 764 (1935).
[23] N. W. Ashcroft, Physical Review Letters **21**, 1748 (1968).
[24] D. A. Papaconstantopoulos and B. M. Klein, Ferroelectrics **16**, 307 (1977).
[25] G. D. G. Gyorffy and B. L., Physical Review Letters **28**, 801 (1972).
[26] J. M. McMahon, M. A. Morales, C. Pierleoni, and D. M. Ceperley, Reviews of Modern Physics **84**, 1607 (2012).
[27] W. Pickett and M. Eremets, Physics Today **72**, 52 (2019).
[28] M. Somayazulu, M. Ahart, A. K. Mishra, Z. M. Geballe, M. Baldini, Y. Meng, V. V. Struzhkin, and R. J. Hemley, Physical Review Letters **122**, 027001 (2019).
[29] C. Wang, S. Yi, and J.-H. Cho, Physical Review B **100**, 060502(R) (2019).
[30] Y. Quan, S. S. Ghosh, and W. E. Pickett, Physical Review B **100**, 184505 (2019).
[31] D. J. Singh, *Planewaves, Pseudopotentials, and the LAPW Method* (Kluwer Academic, Boston and London, 1994).
[32] O. K. Andersen, Physical Review B **12**, 3060 (1975).
[33] L. Hedin and B. I. Lundqvist, Journal of Physics C: Solid State Physics **4**, 2064 (1971).
[34] W. L. McMillan, Physical Review **167**, 331 (1968).
[35] J. J. Hopfield, Physical Review **186**, 443 (1969).
[36] P. B. Allen and R. C. Dynes, Physical Review B **12**, 905 (1975).
[37] B. M. Klein and D. A. Papaconstantopoulos, Journal of Physics F: Metal Physics **6**, 1135 (1976).